

Shear sense analysis of the Higher Himalayan Crystalline Belt and tectonics of the South Tibetan Detachment System, Alaknanda–Dhauli Ganga valleys, Uttarakhand Himalaya

M. Shreshtha¹, A. K. Jain^{2,*} and Sandeep Singh¹

¹Department of Earth Sciences, Indian Institute of Technology, Roorkee 247 667, India

²CSIR-Central Building Research Institute, Roorkee 247 667, India

In the central parts of Uttarakhand Himalaya, more than 20 km thick homoclinally NE-dipping Higher Himalayan Crystalline (HHC) Belt is thrust over the Lesser Himalaya Sedimentary Belt along the Main Central Thrust (MCT), and is almost continuously exposed between Helang and Malari along the Alaknanda and Dhauli Ganga valleys. The upper contact of this belt with the Martoli Formation of the Tethyan Himalayan Sequence is demarcated by the South Tibetan Detachment System (STDS). The belt is ubiquitously marked by small-scale asymmetrical structures like S–C and S–C' foliation, porphyroclasts and porphyroblasts, mineral fishes, intrafolial folds, duplex structures, ductile–brittle shear zones, and asymmetric shear boudins. Sense of ductile to brittle–ductile shearing has been determined from these structures across the whole belt, the MCT and the STDS, and reveals two phases of shear deformation: (a) an older top-to-SW upwards phase throughout the HHC, having an overall thrust geometry (DS1), and (b) a younger superposed top-to-NE downwards phase with normal fault sense from the middle to upper parts (DS2). These shear senses provide invaluable constraints on various tectonic models currently in use for the evolution of the Himalayan metamorphics.

Keywords: Higher Himalayan Crystalline Belt, shear structures, tectonic models.

THE India–Asia convergence since ~55 Ma has remobilized and deformed the Proterozoic crust along the northern margin of the erstwhile Indian subcontinent and dismembered it into numerous tectonic zones of regional dimensions such as the South Tibet Detachment System (STDS), Main Central Thrust (MCT), Vaikrita Thrust (VT), Main Boundary Thrust (MBT) and Main Frontal Thrust (MFT)^{1–5}. This crust presently occurs as an extensive Himalayan Metamorphic Belt (HMB) as a consequence of an initial continental subduction to produce ultrahigh pressure Tso Moriri Crystalline (TMC) Belt in

the northeast, the Higher Himalayan Crystalline (HHC) Belt and its Tethyan cover in the middle and the Jutogh nappe (the Lesser Himalayan metamorphic nappes) in the south.

The STDS was first recognized in southern Tibet within the contractional Himalayan orogen, having top-to-north downward movement sense in contrast to the southward thrusting along the MCT^{6,7}. Since then it has been documented almost everywhere along the strike of the Himalayan belt from western Himalaya to Nepal and Bhutan^{4,8–19}. Initially, it was also identified as a thrust by the Chinese researchers²⁰.

The STDS corresponds to a series of north-dipping structures accommodating top-to-north normal motion of the Tethyan Himalayan Sequence (THS) in southern Tibet with respect to the underlying HHC Belt^{6,10}. The STDS is also known as the Zaskar Shear Zone⁹, Rohtang Shear Zone¹⁵, Trans-Himadri Fault^{21,22}, Dar-Martoli Fault²³ and North Himalayan Normal Fault²⁴. The description of the Zaskar Shear Zone as a NE-dipping normal fault by Herren⁹ is similar to the faults in southern Tibet⁶. However, it also exhibits both ductile and brittle shear senses with top-to-southwest overthrust and top-to-northeast normal sense of movements^{11,25}, separating the highly metamorphosed Zaskar metamorphics from the overlying slightly metamorphosed late Precambrian to Early Cambrian Phe Formation⁹.

In southern Tibet, normal slip has occurred on several parallel low-dipping structures along the STDS that exhibit from top to bottom: (i) a few brittle normal faults in the THS, (ii) a detachment between THS and the underlying metamorphic belt, and (iii) the STDS ductile shear zone at the top of the HHC, having highly deformed gneisses with NE-trending lineation and numerous shear structures indicating normal slip²⁶.

The extension associated with the STDS was initially attributed to gravitational collapse of the Himalayan topographic front during crustal thickening^{8,10,27}. The STDS and MCT are used to model the movement of the HHC either as a (i) southward-moving crustal wedge^{6,8,12,13,28,29}, or (ii) defining the base and top of a low-viscosity channel

*For correspondence. (e-mail: himalfes@gmail.com)

flow expelled from beneath the Tibetan plateau within the lower crust^{30,31}, or (iii) accommodating the southward extrusion of the HHC^{32–34}.

This article documents various ductile and brittle–ductile shear structures across one of the most accessible and continuous cross-sections of the HHC between the MCT at the base and the STDS at its top along the Alaknanda–Dhauliganga valleys in the central part of the Uttarakhand Himalaya. These structures are then analysed in deciphering shear movements across the HHC and the role of the STDS in the overall tectonic model.

Geological setting

Along the Alaknanda–Dhauliganga valleys of central Uttarakhand Himalaya, the HHC Belt represents more than 20 km thick homoclinal NE-dipping crystalline core of the orogen, bounded by the MCT at its base, and the STDS^{1,2,18,22,35–41} near its top (Figure 1*a*). This belt is thrust southwards over the very low-grade metamorphosed Proterozoic Lesser Himalayan sedimentary belt (LH) at its base along the MCT, as was originally recognized by Heim and Gansser³⁵ in this very section.

Two thrusts bound an imbricated Munsiri Group of rocks within the MCT ductile shear zone at the base of the HHC: the Munsiri Thrust (MT) at its lowermost part of the section and the Vaikrita Thrust (VT) at the top

(Figure 1). Though lithological, structural and isotopic criteria have been used to decipher whether the MT or VT defines the actual MCT^{1,35,40–44}, according to the present authors the southernmost boundary of this metamorphic belt, defining the most distinct boundary, should be treated as the MCT, as was originally defined by Heim and Gansser³⁵.

The lowermost parts of the HHC contain a highly imbricated and mylonitized Paleoproterozoic low to medium-grade Munsiri Group of rocks of dominant mylonitic augen gneiss (²⁰⁷Pb/²⁰⁶Pb zircon age of 1848 ± 5 Ma from Jharkula, about 10 km west of Joshimath on the main Rishikesh–Joshimath road and 1830 ± 6 Ma age from Tapovan (Locality 7)⁴⁴) and fine-grained biotite-rich gneiss, garnetiferous mica schist, phyllonite, sheared amphibolite and a persistent imbricated horizon of sericite-bearing sheared and foliated quartzite; the latter bears a strong lithological resemblance with the Lesser Himalayan Berinag Group quartzite (Figure 1*a*). It is likely to have been incorporated within the basement Munsiri-type of rocks due to imbricated Lesser Himalayan rocks. The overlying Vaikrita Group is divided into three formations: (i) the lower Joshimath Formation of garnetiferous biotite–muscovite schist and psammitic gneiss, (ii) the middle Surathota Formation containing banded and flaggy psammitic gneiss, kyanite–garnet–biotite gneiss/schist and amphibolite, and (iii) the upper Bhapkund Formation of sillimanite (fibrolite)–kyanite–garnet–biotite gneiss/schist, psammitic gneiss/schist with pervasive migmatite, concordant to discordant pegmatite veins and small, tourmaline-rich leucogranite lenses/dykes and the Malari leucogranite. Structural control on five distinct phases of melt accumulation has been identified in this formation where stromatolite layers and concordant leucogranite bands, paralleling the main foliation S_m , mark the oldest migmatite phase Me1 (ref. 41). Superposed Me2, Me3 and Me5 younger melt phases are along small-scale ductile thrusts, extensional fabric and structureless patches respectively, while the Me4 melting phase is only evidenced by large-scale migration along cross-cutting irregular veins as possible melt conduits for migration and accumulation into larger leucogranite bodies like the Malari granite (19.0 ± 0.5 Ma)³⁹. Within the HHC, the Malari leucogranite is a narrow and poorly exposed body, which is unmappable on 1:50,000 scale. About 200 m wide exposure of deformed megacrystic granite gneiss occurs between the Malari village and a bridge on the road approaching the village, and is intruded by leucogranite small sills and dykes³⁹.

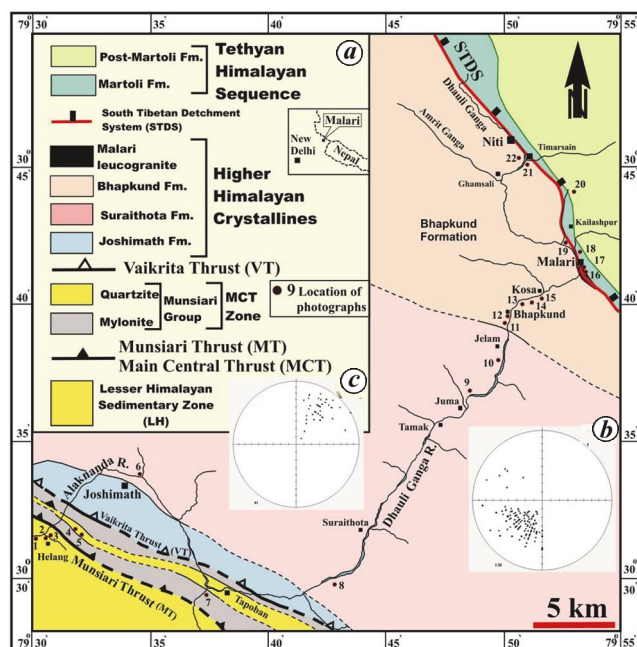


Figure 1. *a*, Geological map of the Higher Himalayan Crystalline Belt along the Alaknanda–Dhauliganga Valleys. (Source: authors' observations and published literature.) *b*, Orientation data of 41 lineations developed on main foliation S_m plotted equal area projection using GEORient. *c*, Orientation data of 138 main foliation S_m , plotted on equal area projection using GEORient. Location of photographs used in this article are shown as latitude and longitude, and our original field locations in bracket.

Martoli Formation

The basal THS is best exposed around the village Malari as the Martoli Formation, which dominantly contains grayish-green slate and quartzite. Overall dip of the Martoli is due N-to-NE.

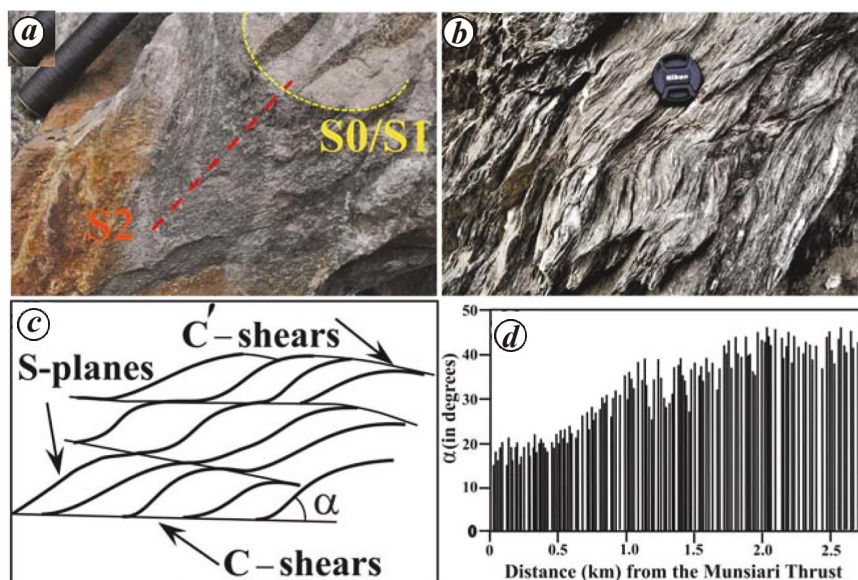


Figure 2. Characters of various kinds of foliations from the HHC. *a*, Tight fold on psammite/pelite alternations S0/S1 (lithological banding) and development of intense axial plane foliation S2 near Helang. Loc. 1: 30°31'42" : 79°32'03" (RM 45). Scale: Hammer head. *b*, S-C and C' shear fabrics within schist of the Munsiri Thrust zone near Helang. Note top-to-SW upwards thrust geometry of planes. Top of photograph points SW. Loc. 2: 30°31'40" : 79°30'08" (RM 36). *c*, Idealized diagram of S-C and C' shear fabric and angle α between S and C planes. *d*, Measurements of angle α ($n = 132$) within the MCT thrust zone. Distance measured from surface trace of the Munsiri Thrust.

Shear sense indicators within the HHC

The HHC incorporates a very large component of late Paleoproterozoic metamorphics⁴⁴ and relict structures such as rare, isolated, tight and 'flame-type' F1 folds on lithological banding and/or metamorphic layering (S0), representing the D1 deformation phase¹⁵. However, the most prominent, intense and widespread deformation D2 is characterized by penetrative foliation (S2), which parallels the axial surfaces of tight to isoclinal reclined to recumbent F2 folds on S0/S1 foliation (Figure 2 *a*). In the absence of fold hinges of these folds, all these foliations become indistinguishable from each other and are grouped as the main foliation (S_m ; Figure 1 *b*). Like other parts of the HHC in NW Himalaya, the S2 foliation has undergone extreme flow due to ductile shearing and becomes essentially a composite S-C planar shear fabric with regional NW-SE trend and NE dips^{11,45} (Figure 2 *b*). Measurements of angle between S and C planes indicate that it decreases from 45° to 15° within the MCT shear zone (Figure 2 *c* and *d*). This superposed ductile shearing along the S2 foliation has resulted in transposition and obliteration of all the earlier planar structures. Extensive flow within the HHC has developed a prominent L2 stretching lineation (Figure 1 *c*). Such a deformation pattern is not only confined to the HHC, but extends to the STDS, the overlying THS cover to the Proterozoic basement, the MT and VT zones, and footwall of the Lesser Himalayan Sedimentary Zone^{11,15,46-48}.

During subsequent superposed D3 deformational phase, close to isoclinal recumbent to gently inclined F3 folds

on earlier S1-S2 and/or C-foliation, axial plane crenulation foliation (S3) and L3 mineral lineation are developed parallel to the Himalayan orogen; the F3 folds sometimes produce very large folds in Zaskar and Himachal Pradesh. Kink bands, tension gashes, slickensides and joints are developed on earlier foliations during D4 deformation. One of the important features of the D4 event is the presence of large-scale open and upright cross-folds that produce culminations and depressions, and control outcrop patterns of many tectonic units.

As a consequence of non-coaxial deformation within the whole HHC belt along the Alaknanda-Dhauliganga valleys from Helang to Malari-Niti, a number of asymmetric, small-scale deformational structures provide extremely useful and invaluable information regarding the direction of tectonic transport and evolution of this belt. Most useful shear sense indicators in this belt are the S-C and S-C' fabrics, asymmetric porphyroclasts and porphyroblasts, mineral fishes, asymmetric boudins and duplex-type shear zones. From the asymmetry of the structures shear sense was determined in the field and from oriented thin sections in planes perpendicular to the main foliation and paralleling the stretching lineation (XZ plane).

S-C and S-C' foliation

Shear bands or C-surfaces are shear foliation that transects a well-developed simultaneous foliation S at a small angle, and the combined texture is called a shear band foliation or S-C foliation/fabric^{49,50} (Figures 2 and 3).

The S-surfaces become sigmoidal in character and gradually deflect near the C-surfaces paralleling the main shear zone. Sense of shear is determined from acute angle between the S- and C-foliations (Figures 2 *c* and 3 *a* and *b*). Within the HHC S–C fabrics are developed both in the granite mylonite and psammitic gneiss/schist where C-fabric is superposed upon the S-fabric and both are distinguishable (Figure 3 *a*). At other places within the MCT zone, the C-fabric dominates over the S-fabric or foliation is mainly marked by C-plane with S-plane denoting the pre-existing foliation (Figure 3 *a*).

C'-foliation, described originally as C'-bands⁵¹ or extensional crenulation cleavage (ecc)⁵², is observed within the HHC as oblique discrete bands causing sigmoidal curvature of S-planes. C'-planes make angles of 15–35° with the main C-shears (Figure 2 *a* and *b*). These are usually later than the S–C-fabric and more weakly developed, shorter and wavy than the C-planes. One set of C'-shears is commonly developed at low angle and exhibits the same sense of movement as the C-shears (synthetic) or may also show opposite dip (antithetic) and shear sense as the C''-shears.

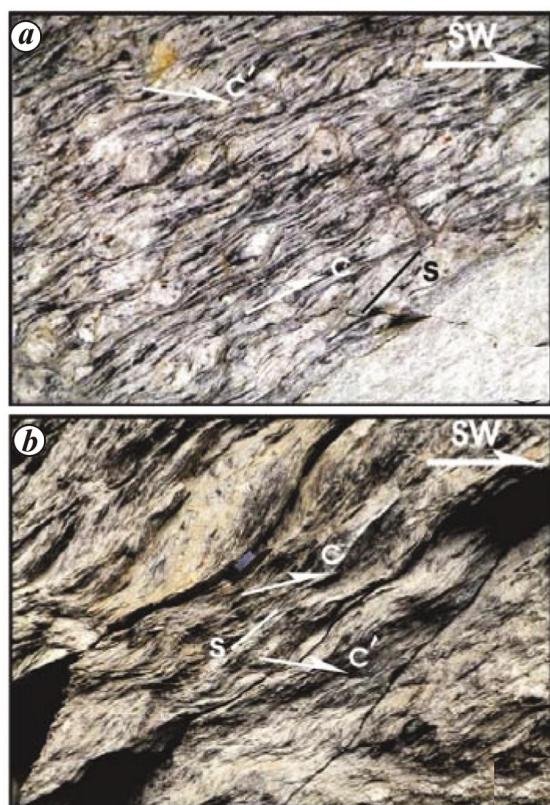


Figure 3. S–C and C' shear fabric/foliation as top-to-SW (thrust) shear sense indicators from the HHC metamorphic. *a*, S–C and C' shears within the porphyroclastic granite mylonite of the MCT zone of the Munsiri Group west of Tapovan along the Dhak Nala. Loc. 7: 30°31'28" : 79°37'28" (RM 68). Scale: Width of photograph is 12 cm. *b*, Schist of the Munsiri Thrust zone (MCT) near Helang with subparallel S–C fabric. Loc. 3: 30°31'32" : 79°30'30" (RM 35). Scale: Width of photograph is about 20 cm.

Porphyroclasts

Relict, more rigid porphyroclasts within the HHC of these valleys consist of a central sigmoidal-shaped single crystal within highly sheared, fine-grained, foliated matrix (Figures 3 *a* and 4 *a*). They typically develop from more resistant feldspar in a strongly foliated quartz, feldspar and mica matrix in sheared granite mylonite. During the course of deformation, the porphyroclasts develop asymmetric recrystallized tails showing stair-stepping geometry (Figure 3 *a*). The most common is σ -type, whose asymmetry and stair-stepping define the shear sense (Figures 3 *a* and 4 *a*). Rarely δ -type tails are also seen; both of them are useful in shear sense determination.

Porphyroblasts

Syntectonically growing, asymmetrical garnet and feldspar porphyroblasts are recorded from the kyanite-bearing garnetiferous mica gneiss/schist of the Surathota and Bhapkund Formations within the HHC, while migmatite from the latter formation contains porphyroblastic feldspar (Figure 4 *b–d*). Reaction rims of mafic and feldspar–quartz mineral aggregates in the Bhapkund Formation of the HHC may be classified as mantled porphyroblasts (Figure 4 *d*), having sigmoidal inclusion trails of other minerals, and are themselves bounded by the S–C foliation.

Sigmoidal shapes of numerous quartz and mica inclusion trails, trapped inside the porphyroblasts during their growth and simultaneous rotation, provide the evidences of top-to-SW (thrust) shear sense.

Mineral fish

The HHC exhibits numerous instances of asymmetrical, elongate, sigma-shaped mineral fish in a fine-grained matrix along these valleys (Figure 5 *a* and *b*). The most commonly observed fishes are of feldspar, quartz and white mica (Figure 5 *a* and *b*)⁵⁰. Mica fishes are lenticular in shape and belong to Group 1 and Group 2 (ref. 53; Figure 5 *b*). Rarely, asymmetrical garnet porphyroblasts also form elongate fishes (Figure 4 *b*).

At places lenticular polycrystalline aggregates of fine mica flakes preserving an earlier shear fabric form the fishes (Figure 5 *c*); these are designated as foliation fish or tectonic fish.

Duplex structure

Rare duplex structures are observed within the HHC, where low-angle floor and roof thrusts linked by ramps bound 'lozenge'-shaped rock masses due to overlapping characters of thrust surfaces (Figure 5 *d*). Duplex structures of both the contractional and extensional regimes

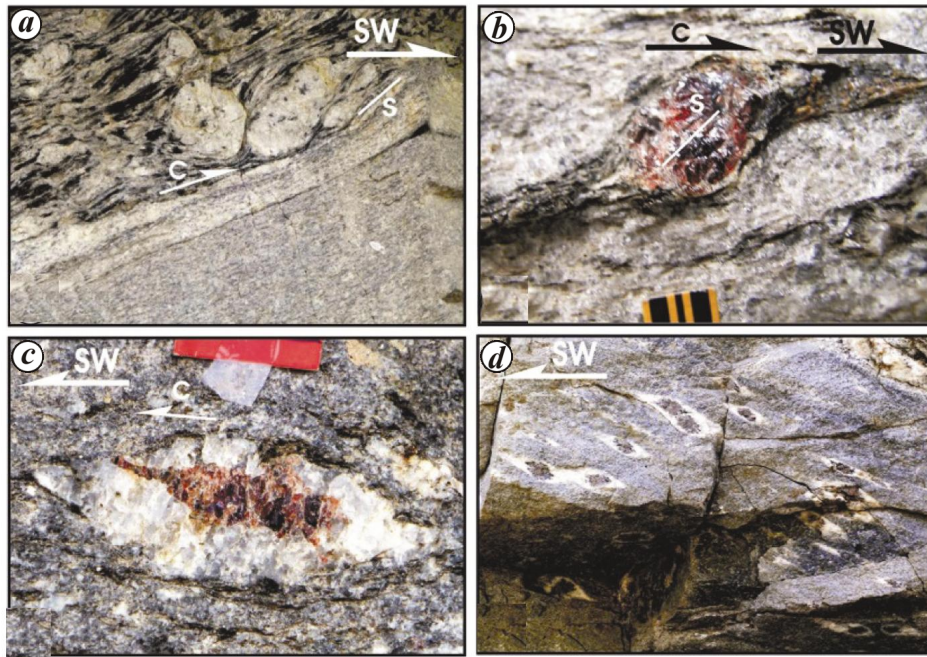


Figure 4. Asymmetrical porphyroclast and porphyroblast systems in the HHC showing top-to-SW upward thrust shear sense. *a*, Large feldspar porphyroclast within granite mylonite of the Munsiri Group, MCT zone, west of Tapovan along the Dhak Nala. S–C shear fabric is also seen having same shear sense. Loc. 7: $30^{\circ}31'28'' : 79^{\circ}37'28''$ (RM 68). Scale: Photograph width is about 10 cm. *b*, Winged garnet porphyroblast in sillimanite–kyanite–garnet gneiss within Bhapkund Formation after crossing the Bhapkund bridge. Loc. 15: $30^{\circ}40'15'' : 79^{\circ}50'10''$ (RM 10). Scale: 1 cm. *c*, Tailed garnet porphyroblast in kyanite–garnet gneiss within the Suraithota Formation at Vishnuprayag. Loc. 6: $30^{\circ}33'54'' : 79^{\circ}34'36''$ (RM 48). Scale: 2 cm. *d*, Garnet porphyroblasts with asymmetrical rim of feldspar–quartz in the Bhapkund Formation of the HHC near Bhapkund. Loc. 11: $30^{\circ}39'31'' : 79^{\circ}50'0''$ (RM 95). Scale: Photograph width is about 8 cm.

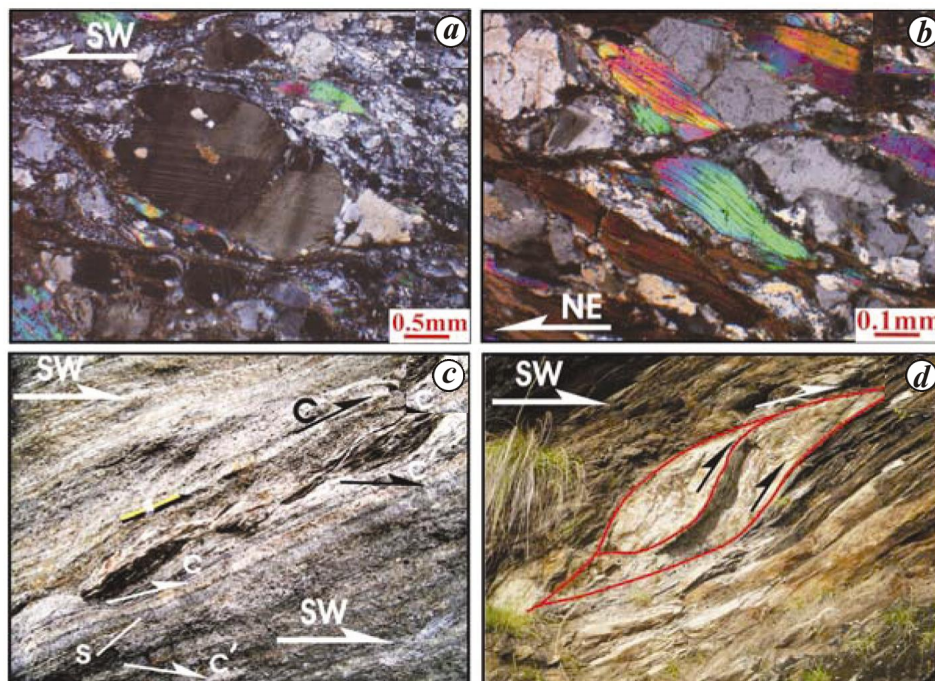


Figure 5. *a, b*, Photomicrographs of the feldspar, quartz and muscovite fish from the mylonitized gneiss of the HHC along the STDS at Timarsain. Loc. 21: $30^{\circ}45'47'' : 79^{\circ}51'00''$ (RM 20). *c*, Foliation fish formed by isolated lens-shaped polycrystalline mica aggregates preserving an earlier shear fabric from the MCT zone near Helang. Loc. 1: $30^{\circ}31'37'' : 79^{\circ}30'00''$ (RM 34). Scale: 4 cm. *d*, Duplex structure having top-to-SW shear sense in mica schist of the MCT zone near Helang. Loc. 4: $30^{\circ}31'52'' : 79^{\circ}31'47''$ (RM 39). Scale: Width of photograph: 1 m.

were observed; the former are located within the MCT zone, while the latter are seen within the STDS zone.

Intrafolial folds within ductile shear zones

Several kinds of folds characterize the ductile shear zones within the HHC and are useful in determining their shear sense. Of these, intrafolial asymmetrical folds are most common (Figure 6), and develop due to folding of the pre-existing layers and their transposition during ductile shearing. When combined with other criteria, these become a strong tool for deciphering the shear sense within the HHC.

Non-cylindrical sheath folds with strongly curved and bent back hinges⁵⁴ also characterize the ductile shear zones within the HHC, especially the MCT zone. The interlimb angle is highly reduced, and hinges of the folds are bent like the shape of a ‘hanger’. The convexity of the bent axis points to the direction of shearing and appears to have evolved due to lateral variations of ductile flow. Planar outcrop patterns are highly variable from almost circular to elliptical.

Ductile and brittle–ductile shear zones

Within the HHC of these valleys, isolated ductile to brittle–ductile shear zones are superposed on all the planar structures and display their own shear fabric, which deflects the earlier one into contractional or extensional modes. Of interest are the top-to-SW upwards thrust-type ductile shear zones within the STDS. These make the axial surfaces of tight to isoclinal folds and transpose the axial surfaces of older, tight to isoclinally folded fabric into a new shear fabric (Figure 7a). At many localities quartz veins are sheared by NE-dipping top-to-SW thrust-type shear zones branching up from the main foliation

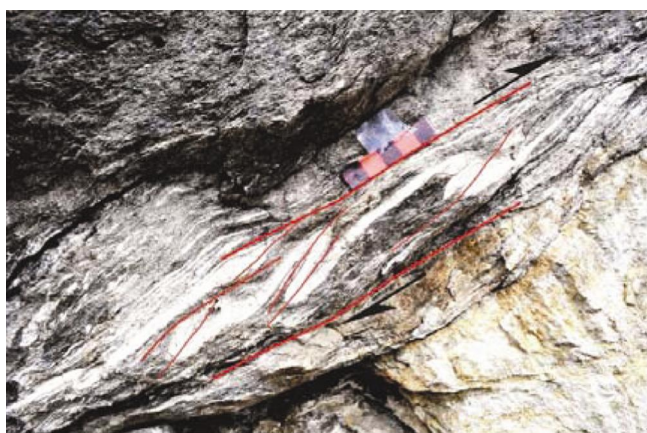


Figure 6. Intrafolial asymmetric folds within the MCT zone, Alaknanda Valley Garhwal. Note gradual rotation of axial surfaces parallel to shear zones. Loc. 5: 30°31'47" : 79°32'03" (RM 45). Scale: 5 cm.

(Figure 7b). On the contrary, extensional ductile shear zones reveal top-to-NE downward movements within migmatite of the upper parts of the Bhapkund Formation, and also contain leucogranite melt (Figure 7c). The STDS is marked by steep NE-dipping steeper brittle–ductile shear zones with top-to-NE sense of movement (normal) near the northernmost exposure of the HHC (Figure 7d).

Asymmetric shear boudins

Rectangular or lozenge-shaped asymmetric boudins, displaced by interboudin surfaces at regular intervals⁵⁵, characterize the HHC in these valleys. The boudins are developed in interbedded rocks of less competent leucogranite and more competent hard gneiss (country rocks) or on quartz veins within pelitic–psammite sequences with both top-to-SW (thrust) shear sense (Figure 8a) and top-to-NE (normal) shear sense (Figure 8b). Both symmetrical and asymmetrical boudins have been identified across the HHC.

V-pull-aparts

In the upper parts of the HHC some rare garnet porphyroblasts are marked by filled ‘V’-shaped gaping cracks, which are asymmetrically oriented and taper downwards (Figure 9a). Individual grains still remain intact, but smaller fragments appear to have moved upwards, and provide indisputable evidence of top-to-SW (thrust) shear sense⁵⁶.

Asymmetrical folds

The whole of the HHC displays a variety of F2/F3 folds whose asymmetry reveal top-to-SW upwards shear sense in the lower parts. However, the upper part of the HHC, mainly in the Bhapkund Formation, is characterized by asymmetrical tight to isoclinal folds whose vergence changes and indicates top-to-NE downwards shear sense (Figure 9b).

Structures of the South Tibetan Detachment System

The STDS separates the low-grade Martoli Formation of the THS from the high-grade Bhapkund Formation of the HHC (Figures 1 and 10). Near Malari, it consists of a 1–2 km wide ductile shear zone with typical fine-grained mylonite/ultramylonite and is overprinted by discrete brittle–ductile and brittle fracture zones that dip variably and are 0.5–30 m thick (Figure 11).

Peak metamorphic temperature calculated from mineral equilibria remains nearly constant (800–850°C)

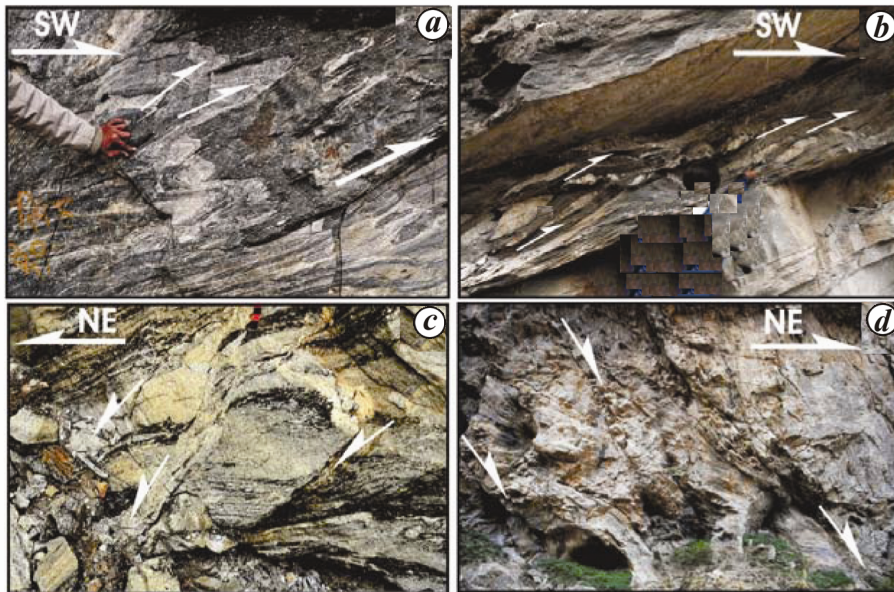


Figure 7. Ductile to brittle–ductile shear zones within the HHC. *a*, Top-to-SW thrust-type shear zones within the STDS zone, transposing the older folded fabric along the shear zones before village Kosa. Loc. 14: 30°40'21" : 79°50'19" (RM 9). *b*, Sheared quartz vein train transposed along NE-dipping top-to-SW thrust-type shear zones branching up from the main foliation S_m . Loc. 8: 30°29'45" : 79°43'00" (RM 58) near Surraithota. *c*, Top-to-NE downward shear bands within migmatite, having leucogranite melt near Bhapkund. Loc. 12: 30°39'55" : 79°50'29" (RM 21). Scale: 3 cm. *d*, Steep NE-dipping brittle–ductile shear zones paralleling the STDS. Note the sigmoidal bending of the earlier main foliation. Sense of movement is shown by arrows. North of Malari near Timarsain. Loc. 22: 30°46'00" : 79°49'55" (RM 20A). Scale: Photograph about 10 m.

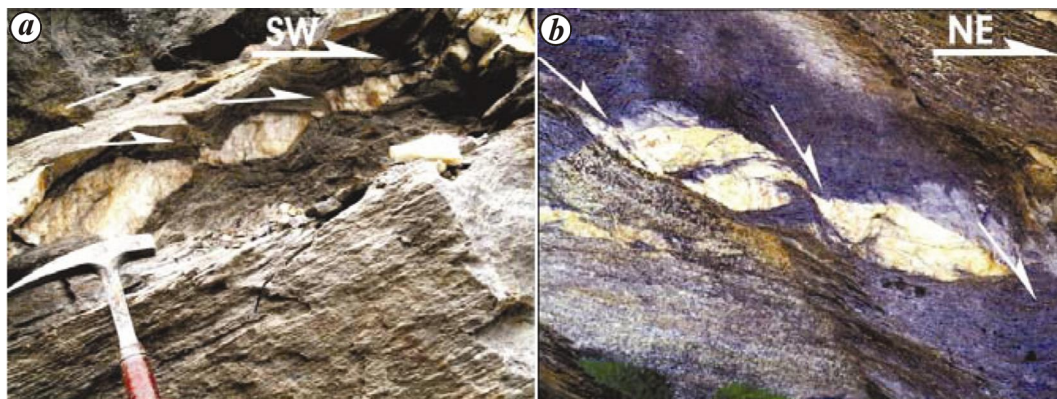


Figure 8. Asymmetrical shear boudins from the HHC. *a*, Series of top-to-SW shear boudins in vein quartz embedded in psammitic schist south of Surraithota. Loc. 8: 30°29'45" : 79°43'00" (RM 58). *b*, Series of fish-mouth shear boudins in vein quartz showing top-to-NE (normal) shear sense near Bhapkund. Loc. 9: 30°36'14" : 79°48'11" (RM 26).

throughout the HHC up to the STDS. However, peak metamorphic pressures increase from 12 to 14 kbar 3 km above the VT and then decrease to 9 kbar at the STDS⁴⁰. Thus, the HHC belt is typically characterized by inverted metamorphism with development of sillimanite–K-feldspar gneiss and migmatite in the uppermost parts of the Bhapkund Formation.

Brittle structures like normal faults and conjugate fractures increase in frequency up section toward the STDS. Most orogen-parallel normal faults strike subparallel to the STDS and have minor displacements (<10 m) with mostly top-to-NE downward motion⁴⁰.

From the Malari village, a picturesque view of the STDS contact between the steeply-dipping HHC and the gentle THS is available and depicts the overall tectonics of this fault (Figure 11 *a, b*). As one crosses the Malari village going further northwestward, one can observe normal faults (Figure 11 *b, c*) and their fault gouge zones and intense pulverization (Figure 11 *c*) due to brittle deformation by the STDS. Extensional shear bands also affect the Martoli Formation and have top-to-NE downward normal shear sense (Figure 11 *d*).

At the Malari village, rocks on the hanging wall of the extensional STDS acquire listric geometry, especially

granite, which exhibits gentle-dipping ‘apparent’ thrust-type duplexes, possibly due to rollover antiform as a consequence of the extensional movements along the STDS to accommodate the space (Figure 11 e (i) and (ii)). Both types of shear sense indicators were observed within the Malari granite. Close-up observations of the Malari granite exhibit both older top-to-SW upwards structures over which the younger top-to-NE downward structures are superimposed (Figure 11 e (iii) and inset in (ii)).

Observations and discussion

The top-to-SW shear sense indicators are ubiquitously present throughout the HHC. However, kinematic indicators having exclusively top-to-SW shear sense are observed within the Munsiri and Joshimath Formations and continue till the upper parts of the Surraithota Formation. Structures showing top-to-NE shear sense first start appearing in the middle parts of the Surraithota Formation somewhere between Surraithota and Tamak at Location I (30°34’12’’N: 79°44’56’’E; Figure 12). However, shear

structures showing the top-to-SW structures remain the dominant shear fabric and are continuously observed to be dominant up to Tamak village. Between Tamak (Location II – 30°35’49’’N: 79°47’31’’E) and the next village Juma, the zone contains several folds and flow structures along with the first appearance of leucogranite material. However, shear sense indicators are absent throughout this narrow zone. After crossing Juma (Location III – 30°36’7’’N: 79°48’18’’E), kinematic indicators with top-to-NE shear sense become dominant with the appearance of migmatite for the first time. A large migmatite zone is observed after crossing the next village Jelam; the migmatites are ubiquitously distributed up to Malari, but they are observed to be dominant only in the upper parts of the Bhapkund Formation. A few relict structures of top-to-SW shear sense are also observed along with the dominant top-to-NE shear fabric between Bhapkund and Malari. Beyond Malari (Location IV – 30°40’52’’N: 79°53’20’’E), i.e. in the Martoli Formation, we observed exclusively top-to-NE downward shear sense indicators.

On the basis of our field observations and analysis of the shear sense indicators, the whole HHC has been subdivided into the following five zones between Helang and Ghamsali–Niti, including parts of the LHS and the THS (Figure 12). The above classification is based on our shear sense analysis and the simple fact that older phase ductile shear fabric (DS1) or the top-to-SW shear sense indicators represent a compressional/contractual environment, while the younger ductile shear phase fabric (DS2) or the top-to-NE shear sense indicators represent

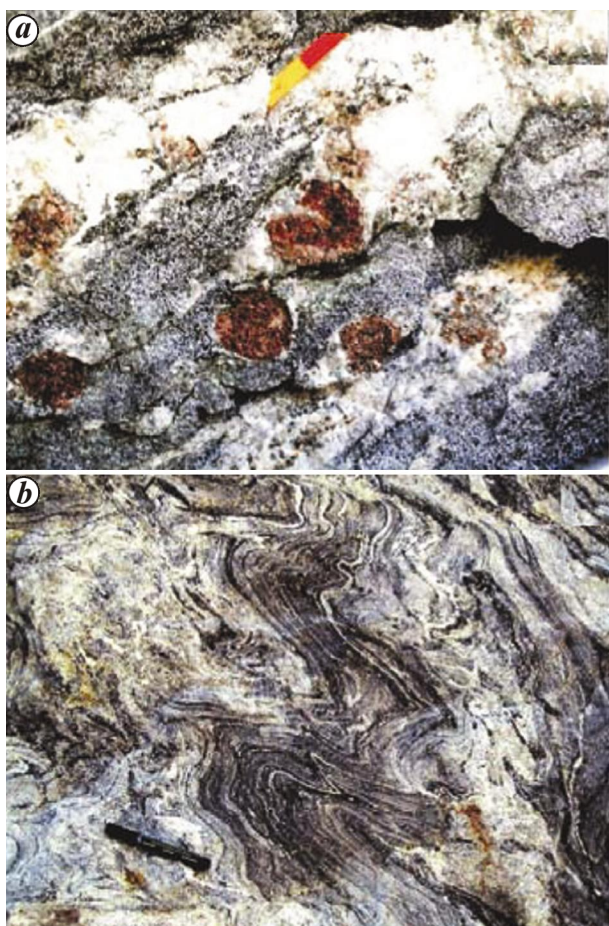


Figure 9. a, ‘V’-pull-apart in garnet from the HHC along the Dhauli Ganga Valley. Loc.: On Bhapkund–Malari Road. Arrow points top-to-SW. Loc. 13: 30°40’10’’: 79°50’47’’ (RM 8). Scale: 2 cm. b, Top-to-NE (normal sense) verging folds in upper parts of the HHC south of Jelam. Loc. 10: 30°38’22’’: 79°49’45’’ (RM 93). Scale: Pen 13.5 cm.

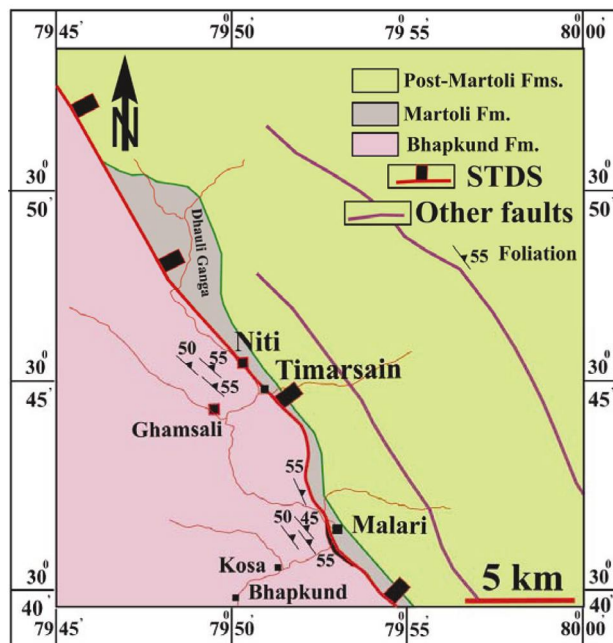


Figure 10. Geological map of the South Tibetan Detachment System (STDS) between Malari and Niti areas showing distribution of different lithologies.

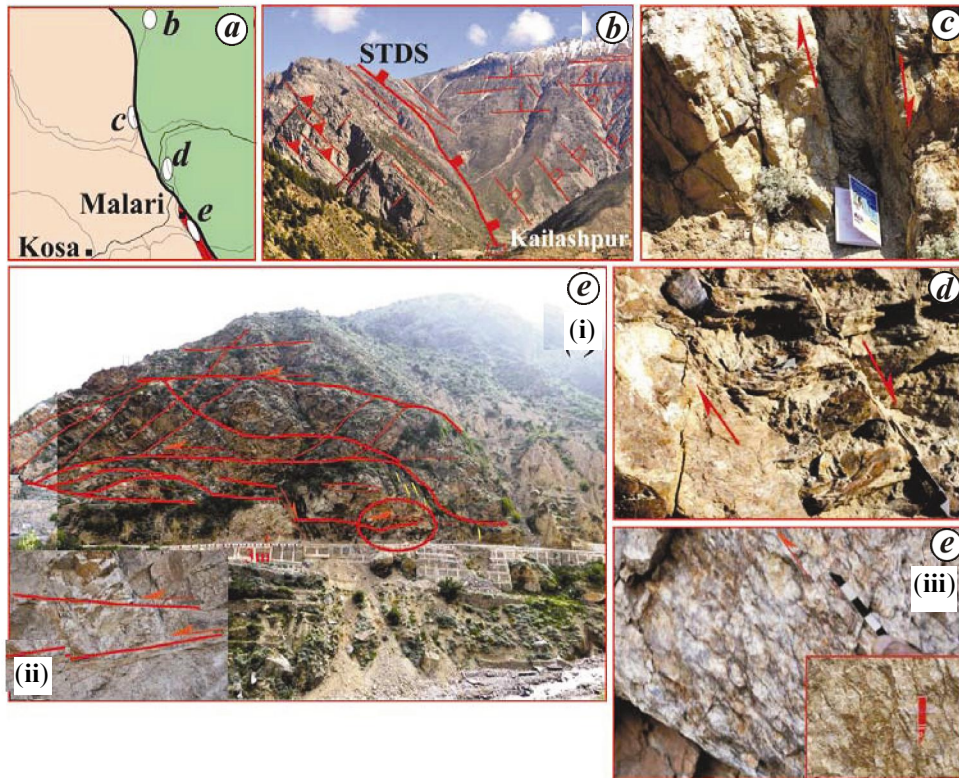


Figure 11. STDS near Malari. *a*, Geological map of the STDS showing various structures in its vicinity of Malari. *b*, The STDS above Kailashpur, observed from Malari. Steeply-dipping HHC gneiss (left) is tectonically overlain by gently-dipping Martoli Formation. Unfilled rectangles indicate small-scale faults. Lines with rectangles are traces of joints. Loc. 20: $30^{\circ}45'00'' : 79^{\circ}53'13''$. *c*, Normal fault and its fault gouge and breccia within leucogranite due to isolated splay extensional fault of the STDS. About 4 km from Malari on the Malari–Niti road. Loc. 19: $30^{\circ}42'32'' : 79^{\circ}52'52''$ (RM 14). *d*, Martoli quartzite deformed by brittle–ductile extensional fault zone near Malari. Loc. 18: $30^{\circ}41'37'' : 79^{\circ}53'00''$ (RM 2). Scale: Pen. *e* (i), Overall fracture pattern in deformed granite with thrusts, normal faults and joints at Malari village. Loc. 17: $30^{\circ}41'00'' : 79^{\circ}53'00''$ (RM A). *e* (ii), (Inset) Details of subhorizontal thrust. *e* (iii) Porphyroclastic Malari granite having asymmetrical megacrysts having top-to-SW (arrow) overthrust sense, and shear bands with top-to-NE downward shear sense on the road near village Malari Loc. 16: $30^{\circ}40'57'' : 79^{\circ}53'45''$ (RM 80). Scale: 5 cm.

an extensional environment. These zones have been mapped as A to E in Figure 12, while observational points of their changes in the field are indicated as I to IV.

(A) Pure contractional zone (PCZ), exhibiting only the DS1 top-to-SW shear phase fabric.

(B) Dominant contractional zone (DCZ), DS2 movement planes with top-to-NE shear sense make their first appearance, but the DS1 fabric remains dominant.

(C) Transition zone (TZ) having no DS1 and DS2 shear sense indicators, but is marked by considerable rock flowage.

(D) Dominant extensional zone (DEZ), in which the DS2 phase shear fabric is dominant over the DS1 phase shear fabric.

(E) Pure extensional zone (PEZ) with only the DS2 phase shear fabric within the THS.

According to the above classification, the PCZ is the zone from the upper parts of the LHS up to the middle parts of the Surraithota Formation; DCZ is the zone accommodating the upper parts of the Surraithota Forma-

tion up to the village Tamak. This zone extends up to approximately 18 km (map distance) from the (VT); TZ is the zone between the villages Tamak and Juma. It starts at a distance of 18 km approximately from the VT and is around 2 km wide; it is the zone starting after the village Juma up to Malari. This zone accommodates upper parts of the Surraithota Formation and the entire Bhapkund Formation. It starts at a distance of 20 km from the VT; PEZ is the zone which accommodates the entire Martoli Formation and starts at a distance of about 30 km from the VT (Figure 12).

Observation of numerous shear sense indicators along these valleys revealed two phases of ductile shear deformation, DS1 and DS2. The later phase DS2 showing top-to-NE downward shear sense was superposed over the older phase DS1 showing top-to-SW upward shear sense. The DS1 indicates that the HHC has been deformed within a broad non-coaxial ductile shear zone of the overthrust type with a consistent top-to-SW sense of movement. It also suggests an early deformation history of the HHC involving large-scale SW-verging ductile shearing

within the Higher Himalayan Shear Zone (HHSZ), associated with the India – Asia continental convergence and compressional tectonics^{11,45}. Though it is difficult to envisage precise relationship between the ductile shearing within the HHSZ and its movement along the MCT, it is likely that the latter represents a zone of high ductile strain. The STDS, on the contrary, is associated with extensional deformation.

The present work highlights the distribution pattern of various kinematic indicators along the Alaknanda–Dhauliganga section and is useful in understanding the evolution of the Himalayan metamorphics within a framework of various recent tectonic models like (i) ductile shearing⁴⁵, (ii) channel flow^{30,31} and (iii) critical wedge/extrusion^{10,29,34}. The ductile shear model postulates consistent top-to-SW thrust shear sense from various kinematic indicators within a broad, ductile HHSZ, where millimetre-scale ductile shearing along S–C shear fabric caused the inverted metamorphism and decompression melting in the upper parts; top-to-NE shear sense near its upper margin remained not so well explained⁴⁵. The channel flow model and its different variants visualize either (i) a pure Couette (or linear) flow between rigid plates where these move relative to one another and produce uniform simple shear across the channel or (ii) a

pure Poiseuille (or parabolic) flow between stationary rigid plates where horizontal gradients in lithostatic pressure and frictional resistance along channel boundaries produce greatest velocities in its centre with decreasing velocities toward the margins, leading to development of opposing shear senses, or (iii) a combination of the two^{57,58} (see also Godin *et al.*¹⁷; references therein). The critical wedge/extrusion models postulate southward extruding metamorphic belt, bounded by the MCT and the STDS at the base and the top respectively^{10,57}.

Shear sense indicators from the HHC belt of the Alaknanda and Dhauliganga valleys can only be explained by a combination of the pure Couette (or linear) flow and pure Poiseuille (or parabolic) flow within either a ductile shear zone or a channel, bounded by the MCT and the STDS, where top-to-SW shear indicators are superposed by the top-to-NE verging structures over a wide zone near the STDS. The Couette (or linear) flow possibly provided top-to-SW shearing throughout the shear zone/channel to start with, and was subsequently superposed by the Poiseuille (or parabolic) flow at a later stage; both the flows would remain indistinguishable from each other in the lower parts of the shear zone/channel. It is only after crossing the Transition Zone that the structures of the Poiseuille flow will start showing up in the shear zone/channel due to their opposite vergence.

Conclusions

Various small-scale ductile to brittle shear structures such as S–C and S–C' shear fabric, porphyroclasts and porphyroblasts, mineral fish, asymmetric boudins, duplex and shear zones have been used for deciphering the shear sense within the HHC along the Alaknanda and Dhauliganga valleys of Uttarakhand Himalaya. This analysis revealed crucial information regarding two phases of ductile shear deformation, DS1 and DS2, where DS1 is the older phase of SW-verging shearing associated with the compressional tectonics, and DS2 is the younger phase of late orogenic NE-verging normal faulting/shearing. On close examination of these structures, five distinct zones have been mapped in this section: (i) PCZ with only the DS1 shear fabric, (ii) DCZ with DS1 fabric dominating over the DS2 phase, (iii) TZ with extensive flowage having no shear sense indicators, (iv) DEZ with more frequent DS2 phase dominating over the DS1 phase, and (v) PEZ having only the DS2 phase within the THS. NE-verging extensional ductile shearing is distributed in nearly 20 km wide zone in the Dhauliganga Valley and appears to be unrelated to the STDS shear fabric, which appears to be highly localized in character. These fabric/kinematic indicators become strong tools in critically assessing various tectonic models like ductile shear, critical wedge and channel-flow models for the evolution of this part of the Himalaya, though quantitative work on strain

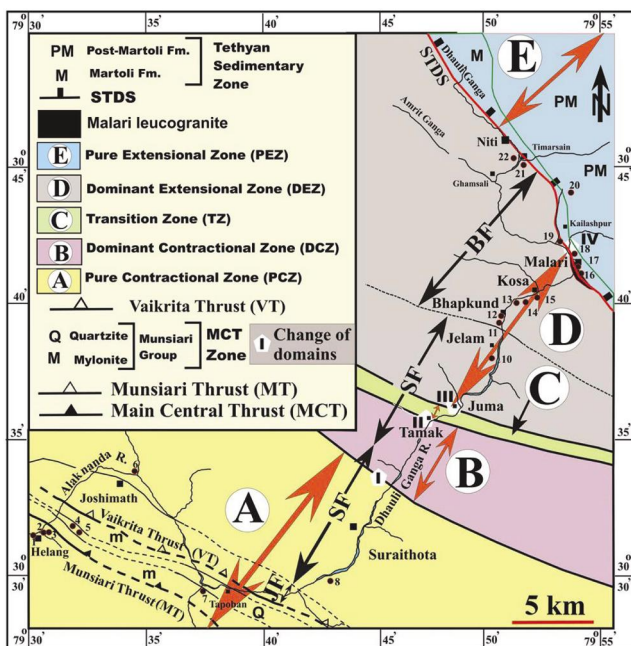


Figure 12. Geological map of the Alaknanda and Dhauliganga Valleys showing distribution of contractional DS1 and extensional DS2 phases of shear structures and their transitions (red arrows) on the basis of shear sense analysis in Uttarakhand Himalaya. Black arrows represent lithological boundaries within the Vaikrita Group. JF, Joshimath Formation; SF, Surraithota Formation; BF, Bhapkund Formation. Note: domain boundaries of the DS1 and DS2 shear structures and their transitions transgress the lithological boundaries. Change of domains indicated by I to IV. Locations of photographs used in this article are also shown.

and metamorphic gradients is required to precisely select the model for the evolution of the HHC. Our preferred model for the evolution of this part of the Himalaya is therefore either a ductile shear zone or a channel in which an older SW-verging ductile shearing associated with the compressional tectonics (the Couette flow) is superposed by the younger DS2 late orogenic NE-verging normal faulting/shearing phase as a consequence of the Poiseuille flow.

1. Valdiya, K. S., *Geology of the Kumaon Lesser Himalaya*, Wadia Institute of Himalayan Geology, Dehra Dun, India, p. 249.
2. Thakur, V. C., *Geology of Western Himalaya*, Pergamon Press, New York, 1993, p. 363.
3. Srikantia, S. V. and Bhargava, O. N., *Geology of Himachal Pradesh*, Geological Society of India, Text Book Series 9, 1998, p. 416.
4. Hodges, K. V., Tectonics of the Himalaya and southern Tibet from two perspectives. *Geol. Soc. Am. Bull.*, 2000, **112**, 324–350.
5. Jain, A. K., Singh, S. and Manickavasagam, R. M., *Himalayan Collision Tectonics*. Gondwana Research Group Memoir, 2002, vol. 7, p. 114.
6. Burg, J. P., Brunel, M., Gapais, D., Chen, G. M. and Liu, G. H., Deformation of leucogranites of the crystalline Main Central Thrust sheet in southern Tibet (China). *J. Struct. Geol.*, 1984, **6**, 535–542.
7. Burg, J. P. and Chen, G. M., Tectonics and structural zonation of southern Tibet, China. *Nature*, 1984, **311**, 219–223.
8. Burchfiel, B. C. and Royden, L. H., North–south extension within the convergent Himalayan region. *Geology*, 1985, **13**, 679–682.
9. Herren, E., Zaskar shear zone: northeast–southwest extension within the Himalayas (Ladakh, India). *Geology*, 1987, **15**, 409–413.
10. Burchfiel, B. C., Chen, Z., Hodges, K. V., Liu, Y., Royden, L. H., Deng, C. and Xu, J., The South Tibet Detachment System, Himalayan orogen: extension contemporaneous with and parallel to shortening in a collisional mountain belt. *Geol. Soc. Am. Spec. Pap.*, 1992, **269**, 1–41.
11. Patel, R. C., Singh, S., Asokan, A., Manickavasagam, R. M. and Jain, A. K., Extensional tectonics in the Himalayan orogen, Zaskar, NW India. In *Himalayan Tectonics* (eds Treolar, P. J. and Searle, M. P.), Geological Society of London, Spec. Publ., 1993, vol. 74, pp. 445–459.
12. Grujic, D., Casey, M., Davidson, C., Hollister, L. S., Kundig, R., Pavlis, T. and Schmid, S., Ductile extrusion of the Higher Himalayan Crystalline in Bhutan: evidence from quartz microfabrics. *Tectonophysics*, 1996, **260**, 21–43.
13. Hodges, K. V., Parrish, R. R. and Searle, M. P., Tectonic evolution of the central Annapurna Range, Nepalese Himalayas. *Tectonics*, 1996, **15**, 1264–1291.
14. Carosi, R., Lombardo, B., Molli, G., Musumeci, G. and Pertusati, P. C., The South Tibetan Detachment System in the Rongbuk valley, Everest region. Deformation features and geological implications. *J. Asian Earth Sci.*, 1998, **16**, 299–311.
15. Jain, A. K., Manickavasagam, R. M. and Singh, S., *Collision Tectonics in the NW Himalaya: Deformation, Metamorphism, Emplacement of Leucogranite along Beas–Parbati Valleys, Himachal Pradesh*. Gondwana Research Group Memoir, 1999, vol. 6, pp. 3–37.
16. Searle, M. P., Simpson, R. L., Law, R. D., Parrish, R. R. and Waters, D. J., The structural geometry, metamorphic and magmatic evolution of the Everest massif, High Himalaya of Nepal–South Tibet. *Geol. Soc. London J.*, 2003, **160**, 345–366.
17. Godin, L., Grujic, D., Law, R. D. and Searle, M. P., Channel flow, ductile extrusion and exhumation in continental collision zones; an introduction. In *Channel Flow, Ductile Extrusion and Exhumation in Continental Collision Zones* (eds Law, R. D., Searle, M. P. and Godin, L.), Geological Society of London, Spec. Publ., 2006, vol. 268, pp. 1–23.
18. Valdiya, K. S. and Pande, K., Behaviour of basement-cover decoupling in compressional deformation regime, northern Kumaun (Uttarakhand) Himalaya. *Proc. Indian Natl. Sci. Acad.*, 2009, **75**(1), 27–40.
19. Kellett, D. A., Grujic, D., Warren, C., Cottle, J., Jamieson, R. and Tenzin, T., Metamorphic history of a syn-convergent orogen-parallel detachment: the South Tibetan detachment system, Bhutan Himalaya. *J. Metamorph. Geol.*, 2010; doi: 10.1111/j.1525-1314.2010.00893.x
20. Academia Sinica, Geological map of Lhasa-Nyalam area, Xizang (Tibet), 1:1500.000. In A Scientific Guidebook to South Xizang (Tibet), 1979, *Academia Sinica*, Beijing.
21. Valdiya, K. S., Trans-Himadri intracrustal fault and basement upwarps south of Indus–Tsangpo Suture Zone. In *Tectonics of Western Himalaya* (eds Malinconico, L. L. and Lillie, R. J.). Geol. Soc. Amer., 1989, pp. 153–168.
22. Valdiya, K. S., Trans-Himadri fault: tectonics of a detachment system in central sector of Himalaya, India. *J. Geol. Soc. India*, 2005, **65**, 537–552.
23. Kumar, G., Mehdi, S. H. and Prakash, G., A review of stratigraphy of part of Uttar Pradesh Tethys Himalaya. *J. Paleontol. Soc. India*, 1972, **15**, 86–98.
24. Pêcher, A., The contact between the higher Himalaya crystallines and the Tibetan sedimentary series: miocene large-scale dextral shearing. *Tectonics*, 1991, **10**, 587–598.
25. Dézes, P. J., Vannay, J. C., Steck, A., Bussy, F. and Cosca, M., Synorogenic extension: quantitative constraints on the age and displacement of the Zaskar shear zone (northwest Himalaya). *Geol. Soc. Am. Bull.*, 1999, **111**(3), 364–374.
26. Leloup, P. H. *et al.*, The South Tibet detachment shear zone in the Dinggye area. Time constraints on extrusion models of the Himalayas. *Earth Planet. Sci. Lett.*, 2010, **292**, 1–16.
27. Hodges, K. V., Burchfiel, B. C., Royden, L. H., Chen, Z. and Liu, Y., The metamorphic signature of contemporaneous extension and shortening in the central Himalayan orogen: data from the Nyalam transect, southern Tibet. *J. Metamorph. Geol.*, 1993, **11**, 721–737.
28. England, P. and Molnar, P., Cause and effect amount thrust and normal faulting, anatectic melting and exhumation in the Himalaya. In *Himalayan Tectonics* (eds Treolar, P. J. and Searle, M. P.), Geological Society of London, Spec. Publ., 1993, vol. 74, pp. 401–411.
29. Grasemann, B., Fritz, H. and Vannay, J. C., Quantitative kinematic flow analysis from the Main Central Thrust Zone (NW-Himalaya, India): implications for a decelerating strain path and the extrusion of orogenic wedges. *J. Struct. Geol.*, 1999, **21**, 837–853.
30. Beaumont, C., Jamieson, R. A., Nguyen, M. H. and Lee, B., Himalayan tectonics explained by extrusion of a low-viscosity crustal channel coupled to focused surface denudation. *Nature*, 2001, **414**, 738–742.
31. Beaumont, C., Nguyen, M., Jamieson, R. and Ellis, S., Crustal flow models in large hot orogens. In *Channel Flow, Ductile Extrusion and Exhumation in Continental Collision Zones* (eds Law, R. D., Searle, M. P. and Godin, L.), Geological Society of London, Spec. Publ., 2006, vol. 268, pp. 91–146.
32. Price, R. A., The southeastern Canadian Cordillera: thrust faulting, tectonic wedging and delamination of the lithosphere. *J. Struct. Geol.*, 1986, **8**, 239–254; doi: 10.1016/0191-8141(86)90046-5
33. Yin, A., Cenozoic tectonic evolution of the Himalayan orogen as constrained by along-strike variation of structural geometry,

- exhumation history and foreland sedimentation. *Earth Sci. Rev.*, 2006, **76**(1–2), 1–131.
34. Webb, A. A. G., Yin, A., Harrison, T. M., C  lerier, J. and Burgess, W. P., The leading edge of the Greater Himalayan Crystallines revealed in the NW Indian Himalaya: implications for the evolution of the Himalayan orogen. *Geology*, 2007, **35**, 955–958; doi: 10.1130/G23931A.1
 35. Heim, A. and Gansser, A., *Central Himalaya: Geological Observations of the Swiss Expedition, 1936*, Memoires de la Soci  t   helv  tique des Sciences Naturelles, 1939, vol. 73, p. 245.
 36. Valdiya, K. S., The extension and analogue of the Chail Nappe in the Kumaun Himalaya. *Indian J. Earth Sci.*, 1978, **5**, 1–19.
 37. Viridi, N. S., Lithostratigraphy and structure of the Central Crystallines in the Alaknanda and Dhauliganga valleys of Garhwal. In *Himalayan Thrust and Associated Rocks* (ed. Saklani, P. S.), Today and Tomorrow's Printers & Publishers, New Delhi, 1986, vol. 10, pp. 155–166.
 38. Gururajan, N. S. and Choudhuri, B. K., Ductile thrusting, metamorphism and normal faulting in Dhauliganga Valley, Garhwal Himalaya. *Himalayan Geol.*, 1999, **20**(2), 19–29.
 39. Sachan, H. K., Kohn, J. M., Saxena, A. and Corrie, S. L., The Malari leucogranite, Garhwal Himalaya, northern India: chemistry, age and tectonic implications. *Geol. Soc. Am. Bull.*, 2010, **122**(11/12), 1865–1876.
 40. Spencer, C. J., Harris, R. A. and Dorais, M. J., The metamorphism and exhumation of the Himalayan metamorphic core, eastern Garhwal region, India. *Tectonics*, 2012, **31**, TC1007, doi: 10.1029/2010TC002853
 41. Jain, A. K., Seth, P., Shreshtha, M., Mukherjee, P. K. and Singh, K., Structurally-controlled melt accumulation: Himalayan migmatites and related deformation, Dhaul Ganga Valley, Garhwal Himalaya. *J. Geol. Soc. India*, 2013, **82**, 313–318.
 42. Gansser, A., *Geology of the Himalaya*. Interscience, New York, 1964, p. 273.
 43. Ahmad, T., Harris, N., Bickle, M., Chapman, H., Bunbury, J. and Prince, C., Isotopic constraints on the structural relationships between the Lesser Himalayan Series and the High Himalayan Crystalline Series, Garhwal Himalaya. *Geol. Soc. Am. Bull.*, 2000, **112**(3), 467–477.
 44. Wiedenbeck, M., Goswami, J. N. and Viridi, N. S., Single zircon $^{207}\text{Pb}/^{206}\text{Pb}$ ages from the Garhwal Himalaya (India): Paleoproterozoic magmatic activity in the Lesser and Higher Himalaya. *Himalayan Geol.*, 2014, **35**, 16–21.
 45. Jain, A. K. and Manickavasagam, R. M., Inverted metamorphism in the intracontinental ductile shear zone during Himalayan collision tectonics. *Geology*, 1993, **21**, 407–410.
 46. Brunel, M., Ductile thrusting in the Himalayas: shear sense criteria and stretching lineation. *Tectonics*, 1986, **5**(2), 247–265.
 47. Mascle, G., P  cher, A., Guillot, S., Rai, S. M. and Gajurel, A., *The Himalayan–Tibet Collision*, Nepal Geological Society, Spec. Publ., 2012, vol. 1, p. 264.
 48. Jain, A. K. and Patel, R. C., Structure of the Higher Himalayan Crystallines along the Suru-Doda valleys (Zaskar), NW Himalaya. In *Geodynamics of the NW Himalaya* (eds Jain, A. K. and Manickavasagam, R. M.), Gondwana Research Group Memoir, 1999, vol. 6, pp. 91–110.
 49. B  rthe, D., Choukroune, P. and Jegouzo, P., Orthogneiss, mylonite and non-coaxial deformation of granites: the example of the South Armorican Shear Zone. *J. Struct. Geol.*, 1979, **1**, 31–24.
 50. Passchier, C. W. and Trouw, R. A. J., *Microtectonics*, Springer-Verlag, 2005, p. 366.
 51. Lister, G. S. and Snoke, A. W., S–C Mylonites. *J. Struct. Geol.*, 1984, **6**, 617–638.
 52. Platt, J. P. and Vissers, R. L. M., Extensional structures in anisotropic rocks. *J. Struct. Geol.*, 1980, **2**, 397–410.
 53. ten Grotenhuis, S. M., Trouw, R. A. J. and Passchier, C. W., Evolution of mica fish in mylonitic rocks. *Tectonophysics*, 2003, **372**, 1–21.
 54. Cobbald, P. and Quinquis, H., Development of sheath folds in shear regimes. *J. Struct. Geol.*, 1980, **2**(1/2), 119–126.
 55. Goscombe, B. D. and Passchier, C. W., Asymmetric boudins as shear sense indicators – an assessment from field data. *J. Struct. Geol.*, 2003, **25**, 575–589.
 56. Hippertt, J. F. M., ‘V’-pull-apart microstructures: a new shear-sense indicator. *J. Struct. Geol.*, 1993, **15**, 1393–1403.
 57. Langille, J., Lee, J., Hacker, B. and Seward, G., Middle crustal ductile deformation patterns in southern Tibet: Insights from vorticity studies in Mabja Dome. *J. Struct. Geol.*, 2010, **32**, 70–85.
 58. Grujic, D., Channel flow and continental collision tectonics: an overview. In *Channel Flow, Ductile Extrusion and Exhumation in Continental Collision Zones* (eds Law, R. D., Searle, M. P. and Godin, L.), Geological Society of London, Spec. Publ., 2006, vol. 268, pp. 25–37.

ACKNOWLEDGEMENTS. This article has emerged from integrated geological studies across a typical cross-section through the Higher Himalaya as a part of the M.Tech thesis by M.S. on the South Tibetan Detachment System, for which he thanks Head, Department of Earth Sciences, IIT Roorkee for providing the necessary facilities. M.S. also thanks the Indian Academy of Sciences for the award of the Summer Fellowship. A.K.J. thanks to the Indian National Science Academy for the Senior Scientist Scheme and Prof. S. K. Bhattacharyya, Director, CSIR-Central Building Research Institute, Roorkee for providing the necessary facilities. We thank P. K. Mukherjee and Kesar Singh (WIHG, Dehra Dun) for lively discussions and interactions in the field. Puneet Seth and Lawrence Kanyan provided field inputs on various occasions. We thank the two anonymous reviewers for comments that helped improve the manuscript.

Received 6 March 2014; revised accepted 22 December 2014